Elastic properties measurement of human enamel based on resonant ultrasound spectroscopy

Haijun Niu, Fan Fan, Rui Wang, Qiang Zhang, Fei Shen, Pengling Ren, Tao Liu, Yubo Fan, Pascal Laugier

Elastic properties measurement of human enamel based on resonant ultrasound spectroscopy

Haijun Niu[a,*], Fan Fan[a], Rui Wang[a], Qiang Zhang[a], Fei Shen[a], Pengling Ren[a], Tao Liu[a], Yubo Fan[a], Pascal Laugier[b]

[a] *Key Laboratory of Ministry of Education for Biomechanics and Mechanobiology, Beijing Advanced Innovation Center for Biomedical Engineering, School of Biological Science and Medical Engineering, Beihang University, Beijing 100083, China*
[b] *Sorbonne Université, INSERM, CNRS, Laboratoire d'Imagerie Biomédicale (LIB), Paris 75006, France*

A R T I C L E I N F O

Keywords:
Biomaterial
Enamel
Elasticity
Resonant ultrasound spectroscopy
Transverse isotropy

A B S T R A C T

Objectives: To investigate the elastic properties of human enamel using resonant ultrasound spectroscopy (RUS).
Methods: Six rectangular parallelepiped specimens were prepared from six human third molars. For all specimens, the theoretical resonant frequencies were calculated using the Rayleigh-Ritz method, knowing the specimen mass density and dimensions, and using *a priori* stiffness constants. The experimental resonant frequencies were measured and extracted by RUS. Then, the optimal stiffness constants were retrieved by adjustment of the theoretical resonant frequencies to the measured ones based on the Levenberg-Marquardt method. The engineering elastic moduli, including Young's moduli, shear moduli, and Poisson's ratios, were also calculated based on the optimal stiffness constants.
Results: The five independent stiffness constants C_{11}, C_{12}, C_{13}, C_{33}, and C_{44} were 90.2 ± 6.65 GPa, 34.7 ± 6.90 GPa, 29.5 ± 4.82 GPa, 83.5 ± 8.93 GPa, and 37.0 ± 10.9 GPa, respectively. Young's moduli E_{11} and E_{33}, shear moduli G_{13} and G_{12}, and Poisson's ratios υ_{12} and υ_{13} were 71.7 ± 7.34 GPa, 69.2 ± 7.32 GPa, 37.0 ± 10.9 GPa, 28.1 ± 4.35 GPa, 0.303 ± 0.098, and 0.248 ± 0.060, respectively.
Significance: Elastic properties are critical for developing dental materials and designing dental prostheses. The RUS method may provide more precise measurement of elastic properties of dental materials.

1. Introduction

Human teeth are primarily composed of enamel, dentin, and dental pulp. Enamel is the hardest and stiffest structure of the human tooth, covering the crown surface and protecting the inner tissue (He and Swain, 2008). Enamel has a multi-level composition of inorganics (mainly hydroxyapatite, about 96% in mass), organics, and water. The basic constituent elements of enamel are enamel prisms, the nano-sized fibril-like hexagonal hydroxyapatite crystals. The shape and arrangement of enamel prisms vary with depth (Cui and Ge, 2007). Enamel is not repairable once it is abraded or damaged. Therefore, alternative materials must be used to repair or rebuild the tooth (Cui and Ge, 2007; Cuy et al., 2002). Understanding the elastic properties and the mechanisms in relation to the compositional and hierarchical microstructure of enamel is critical for developing new approaches to conservative and restorative dentistry.

The methods of measuring enamel elastic properties mainly include conventional macroscopic mechanical testing methods (Bowen and Rodriguez, 1962; Ye et al., 1994; Stanford et al., 1958; Craig et al., 1961) (e.g., stretching and compression), microscopic mechanical testing methods (He and Swain, 2008; Cui and Ge, 2007; Zhang et al., 2014; Habelitz et al., 2001; Zhou and Hsiung, 2006; He et al., 2006) (e.g., nano-indentation), and acoustic methods (e.g., pulse-echo method (Watanabe et al., 2004; Ng et al., 1989), ultrasonic interferometry (Gilmore et al., 1970), and critical angle reflection method (Lees and Rollins, 1972)). While these methods contribute to the understanding of macro- and micro-level elastic properties of enamel, they also have certain drawbacks. For example, macroscopic stretching and compression methods are destructive, and require a relatively large specimen volume, which is difficult to acquire for human enamel (He and Swain, 2008). Nano-indentation is a good method for calculating the micro-scale elastic moduli in different directions for a small-sized specimen, but the results mainly reflect the local elastic properties of the microstructure, which are not necessarily representative of the elastic properties at the macro scale (He and Swain, 2008). Elastic properties can be obtained in a non-destructive manner using ultrasonic methods by

Table 1
Summary of previous research results regarding enamel specimens.

Group	Method	Scale	Source	Shape	Symmetry	Number	Young's Moduli
Ye et al. (1994)	Stretching	Macro-	Human enamel	Rectangular parallelepiped	Isotropic	18	17.29–36.13 GPa
Stanford et al. (1958)	Compression	Macro-	Human enamel	Cylinder	Isotropic	14	62.74–95.84 GPa
Craig et al. (1961)	Compression	Macro-	Human enamel	Cylinder	Isotropic	12	8.27–37.23 GPa
Cuy et al. (2002)	Nano-indentation	Micro-	Human enamel	Surface	Isotropic	3	> 115 GPa
Gilmore et al. (1970)	Ultrasonic interferometry	Macro-	Bovine enamel	Parallel slice	Isotropic	4	32.4–131.0 GPa

measuring the speed of sound, but these approaches require a minimum volume of material with dimensions larger than the wavelength, which can be challenging given the small dimensions of teeth. In addition, obtaining the anisotropic elastic properties requires multiple time-consuming measurements along the main axes of symmetry using both shear and compression sensors (Bernard et al., 2013).

As Table 1 shows, there is no general agreement on the measurement results of enamel elastic properties reported in the literature, particularly for the elastic modulus. Ye et al. measured the elastic modulus of human enamel in the range of 17.29–36.13 GPa by using the stretching method (Ye et al., 1994). Stanford et al. and Craig et al. compressed human enamel specimens and determined their elastic moduli, which ranged from 62.74 to 95.84 GPa and from 8.27 to 37.23 GPa, respectively (Stanford et al., 1958; Craig et al., 1961). Cuy et al. measured the elastic moduli of the human enamel surface to be greater than 115 GPa using the nano-indentation method (Cuy et al., 2002). Gilmore et al. measured the elastic modulus of bovine enamel in the range of 32.4–131.0 GPa using ultrasonic interferometry (Gilmore et al., 1970). Even the same macro-compression methods on the same site did not yield consistent values for the elastic modulus, suggesting that mechanical testing methods are not that accurate (Stanford et al., 1958; Craig et al., 1961). These methods have significant limitations for small-sized brittle materials. Therefore, there is a critical need to develop an accurate method that can be used for these small-sized biomaterials.

Resonant ultrasound spectroscopy (RUS) has been used as an accurate and efficient method to characterize material elastic properties since the 1990s (Migliori and Maynard, 2005; Migliori and Sarrao, 1997; Migliori et al., 1993). The basic principle of an RUS experiment is (1) to measure a series of mechanical resonant frequencies of an object by generating free vibrations with ultrasound excitations, (2) to predict the theoretical resonant frequencies of the object with the Lagrangian variational method using guessed stiffness constants (the forward problem), and (3) to determine the full stiffness tensor of the object by adjusting the stiffness constants until the measured frequencies fit the predicted ones (the inverse problem). RUS is considered as the most accurate method to measure the stiffness constants of high Q (i.e., quality factor) solid materials, such as crystals or rocks. RUS allows all stiffness constants of a small-sized specimen (typically between 1 mm and 1 cm in size, but even less than 1 mm in size) to be measured in a single rapid nondestructive experiment with high reproducibility (Migliori and Maynard, 2005). Recently, Bernard et al. applied RUS with enhanced signal processing methods to highly dissipative materials, such as bone, which broke the limit of the RUS method for measuring stiffness constants of low Q materials (Bernard et al., 2013, 2014, 2015). Kinney et al. measured the elastic properties of human dentin in both the dry and humid states using RUS (Kinney et al., 2003, 2004). Fan et al. used RUS combined with an improved resonant frequency extraction method to estimate the full stiffness constants, as well as engineering elastic moduli, including Young's moduli, shear moduli, and Poisson's ratios, of human dentin specimens (Fan et al., 2017).

RUS has proven to be an effective method for measuring the elastic properties of biological hard tissues, but it has not been applied to measure enamel to date. Our goal was to primarily extend our previous RUS investigation of the elastic properties of human dentin to those of human enamel at the macroscopic level. The results can provide references to understand the structure and function of enamel, to compare the elastic properties of different human dental tissues (e.g., dentin and enamel), and to assist in the design, development, and evaluation of clinical dental restorative materials.

2. Materials and methods

We will not detail here the entire procedure implemented to retrieve the stiffness constants from RUS measurements. It has been described extensively in reports to which the reader may refer (Bernard et al., 2013, 2014, 2015; Migliori and Maynard, 2005; Migliori and Sarrao, 1997; Migliori et al., 1993; Fan et al., 2017). For the sake of clarity, however, we briefly describe hereinafter the main steps. Fig. 1 shows a diagram illustrating the three steps of an RUS experiment. The theoretical resonant frequencies were calculated using the Rayleigh-Ritz method, knowing the specimen mass, its dimensions, and a set of *a priori* stiffness constants. Then, the resonant vibrational modes were ultrasonically excited and the resonant frequencies were extracted from the measured vibrational spectrum. Finally, an iterative numerical procedure, the Levenberg-Marquardt method, was used to adjust the stiffness constants of the model and find the optimal set of stiffness constants for which the theoretical resonant frequencies match the measured ones. Finally, the engineering elastic moduli, including Young's moduli, shear moduli, and Poisson's ratios, were calculated for all specimens based on the optimal stiffness constants.

2.1. Experimental system

Fig. 2(a) contains a schematic of the RUS experimental system. The enamel specimen was mounted on opposing corners between two shear wave transducers (V154RM, Panametrics Inc., U.S.). A network analyzer (Bode 100, OMICRON electronics GmbH, Austria) was used to output a swept-frequency signal as the excitation from the emitter. The resonant signals were amplified by a broadband amplifier (HQA-15M-10T, Femto Messtechnik GmbH, Germany), recorded by the vector

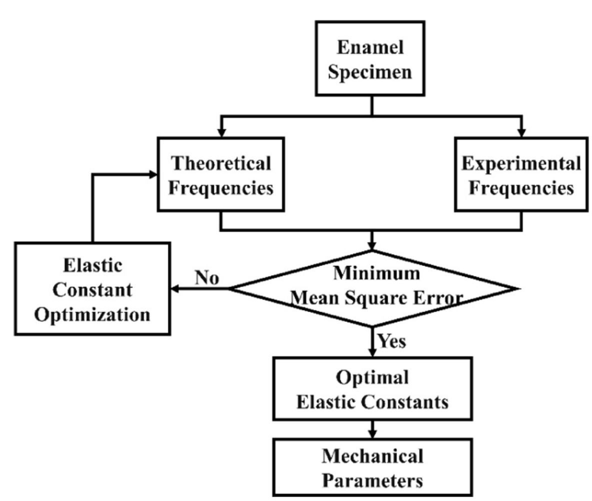

Fig. 1. Flow chart of RUS.

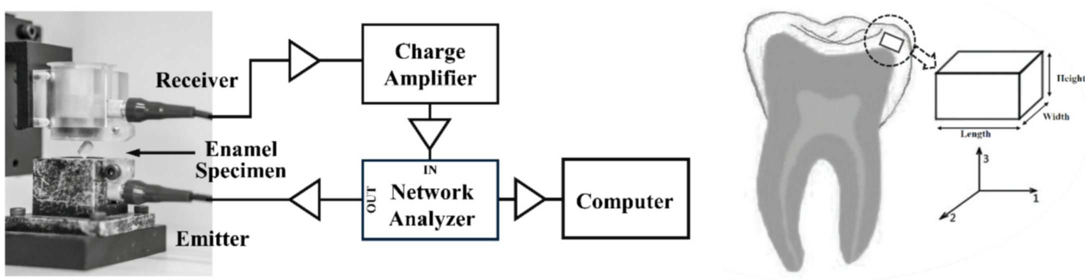

(a) (b)

Fig. 2. Platform of the RUS experiment (a) and sampling of specimen (b).

network analyzer, and imported into a computer for processing.

2.2. Specimen preparations

The specimens used in this study, collected from the Peking University Hospital of Stomatology, consisted of six complete, fresh, and non-carious third molars, removed based on the orthodontic needs of six women aged 25–27 years. Before conducting the experiment, approval was obtained from the Medical Ethics Committee of the administering institution.

After tooth removal, the tartar and granulations were immediately removed from the tooth surface. To roughly cut the occlusal region of the enamel, a low-speed diamond saw (SYJ-150, Shenyang Kejing Auto Instrument Co., Ltd., China) with 0.01-mm positioning accuracy was used, as shown in Fig. 2(b). In order to prepare all specimens with the same orientation and to solve the inverse problem accurately, axis 1 and axis 2 correspond to the two orthogonal axes perpendicular to the main orientation of the enamel prisms and axis 3 corresponds to the axis of symmetry with respect to the main orientation of the enamel prisms, and perpendicular to the tangent direction of the enamel surface. After being polished with 500-grade, 800-grade, and 2000-grade abrasive papers, the standard rectangular parallelepiped specimen was complete. The specimens were stored in saline to maintain a hydrated state prior to experiment. All measurements were made on a fully hydrated specimen.

Mass densities of the enamel specimens were deduced from mass measurements using an electric analytical balance (ME204E, Mettler Toledo, Swiss). They were then scanned by micro computed tomography (micro-CT, SkyScan1076, Bruker Micro-CT N.V., Belgium) at 70 kV, 142 μA, 10 W, Al 1.0 mm filtering, and a voxel size of 9 μm. The images acquired from micro-CT were reconstructed with NRecon software (Bruker Micro-CT N.V., Belgium). The dimensions of the specimens were calculated by Mimics 17.0 (Materialise, Belgium) and are presented in Table 2. Fig. 3(a) shows a photo of a typical enamel specimen and Fig. 3(b) shows the reconstructed model.

2.3. Experimental resonant frequency measurements

The frequency response of the specimen, mounted between two transducers, as shown in Fig. 2(a), was measured by the frequency-sweeping mode with 100 Hz resolution. The frequency-sweeping range was set to include at least the first 30 resonant frequencies. Six independent measurements were performed on each enamel specimen with intermediate repositioning and six groups of experimental resonant frequencies were obtained by seeking local peak amplitude points in the spectra. A typical series of six resonance spectra of one enamel specimen is shown in Fig. 4. The frequencies that occurred at least two times out of six were selected, and their mean values, standard deviations (SD), and coefficients of variation (CV) were calculated. The mean values of the selected frequencies with standard deviations less than 2 kHz and CV less than 0.3% were retained as the experimental resonant frequencies (Bernard et al., 2013).

Table 2
Mass and dimensions of the enamel specimens.

No.	1	2	3	4	5	6
Mass (mg)	51.0	31.0	24.0	30.1	21.1	40.0
Length (mm)	3.68	3.07	2.96	3.24	2.50	3.19
Width (mm)	3.04	1.98	1.88	2.12	1.48	2.86
Height (mm)	1.66	1.87	1.67	1.65	2.24	1.65
Density (mg/mm^3)	2.746	2.727	2.583	2.656	2.546	2.657

2.4. Theoretical resonant frequency calculations

According to the previous calculations using finite element analysis (FEA) (Wen et al., 2014), human enamel is assumed to be a transversely isotropic and inviscid material, with five independent stiffness constants, as shown in (1), where C is the fourth order stiffness tensor.

$$C = \begin{pmatrix} C_{11} & C_{12} & C_{13} & 0 & 0 & 0 \\ C_{12} & C_{11} & C_{13} & 0 & 0 & 0 \\ C_{13} & C_{13} & C_{33} & 0 & 0 & 0 \\ 0 & 0 & 0 & C_{44} & 0 & 0 \\ 0 & 0 & 0 & 0 & C_{44} & 0 \\ 0 & 0 & 0 & 0 & 0 & \frac{1}{2}(C_{11} - C_{12}) \end{pmatrix} \tag{1}$$

Based on the findings of a previous study (Wen et al., 2014), the initial values of the elastic coefficients adopted for this study were deducted to be: $C_{11} = 82.96$ GPa, $C_{12} = 36.04$ GPa, $C_{13} = 34.66$ GPa, $C_{33} = 92.89$ GPa, and $C_{44} = 22.90$ GPa.

The theoretical resonant frequencies of an enamel specimen can be obtained by finding the stationary points of the Lagrangian L given by

$$L = \frac{1}{2}\int\left(\sum_i \rho(2\pi f)^2 u_i^2 - \sum_{i,j,k,l} C\frac{\partial u_i}{\partial x_j}\frac{\partial u_k}{\partial x_l}\right)dV, \tag{2}$$

where ρ is the specimen apparent tissue density, V is the specimen volume, C are initial stiffness constants, f is the resonant frequency, and u_i is the displacement field. The equation was solved by the Rayleigh-Ritz method (Migliori and Sarrao, 1997).

2.5. Stiffness constants

To obtain the final stiffness constants based on the experimental and theoretical resonant frequencies, a cost function $F(C)$ was defined as

$$F(C) = \sum_{i=1}^{N} w_i (f_i^{exp} - f_i^{cal}(C))^2, \tag{3}$$

where f_i^{cal} is the i-th calculated theoretical resonant frequency, f_i^{exp} is the i-th experimental resonant frequency, N is the number of theoretical

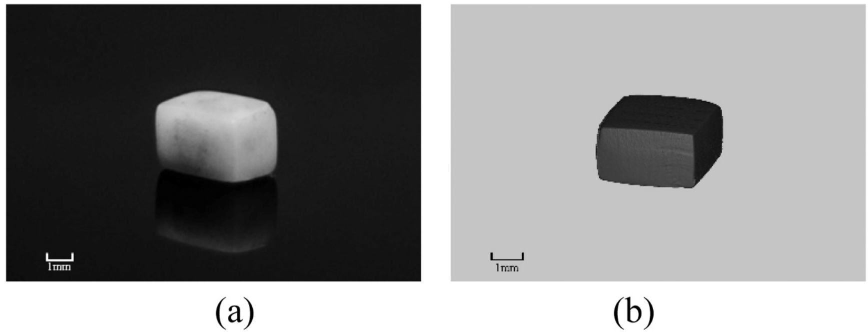

Fig. 3. Photo of a typical enamel specimen (a) and the reconstructed volume (b).

resonant frequencies, C is the stiffness tensor of enamel and, w_i is the weight, given by

$$w_i = \begin{cases} 0 & f_i^{cal} \text{ does not match } f_i^{exp} \\ 1/(f_i^{exp})^2 & f_i^{cal} \text{ matches } f_i^{exp} \end{cases}. \quad (4)$$

Under the convergent condition, the optimal stiffness tensor C was the one that minimized $F(C)$, using the Levenberg-Marquardt method (Bernard et al., 2013).

According to the generalized Hooke's law, the 6 × 6 stiffness tensor was constructed and numerically inverted to obtain the compliance matrix C^{-1}, from which the engineering elastic moduli were calculated.

$$C^{-1} = \begin{pmatrix} 1/E_1 & -\upsilon_{12}/E_1 & -\upsilon_{13}/E_1 & 0 & 0 & 0 \\ -\upsilon_{12}/E_1 & 1/E_1 & -\upsilon_{13}/E_1 & 0 & 0 & 0 \\ -\upsilon_{13}/E_1 & -\upsilon_{13}/E_1 & 1/E_3 & 0 & 0 & 0 \\ 0 & 0 & 0 & 1/G_{13} & 0 & 0 \\ 0 & 0 & 0 & 0 & 1/G_{13} & 0 \\ 0 & 0 & 0 & 0 & 0 & 1/G_{12} \end{pmatrix}, \quad (5)$$

where E_{i} are the Young's moduli (GPa), G_{ij} the shear moduli (GPa), and υ_{ij} the Poisson's ratios (Migliori et al., 1993; Bernard et al., 2014, 2015).

Table 3
Stiffness constants of the enamel specimens.

No.	C_{11} (GPa)	C_{12} (GPa)	C_{13} (GPa)	C_{33} (GPa)	C_{44} (GPa)
1	92.0	26.3	32.7	94.1	29.7
2	96.7	43.5	23.4	72.3	51.9
3	84.8	41.8	29.6	93.8	27.3
4	96.6	30.5	31.9	83.6	32.6
5	80.0	30.1	24.0	76.8	30.7
6	91.3	36.2	35.3	80.3	50.0
Mean	90.2	34.7	29.5	83.5	37.0
SD	6.65	6.90	4.82	8.93	10.9

3. Results

Individual values of the stiffness tensor for all measured specimens are shown in Table 3. The mean values ± SD for C_{11}, C_{12}, C_{13}, C_{33}, and C_{44} are 90.2 ± 6.65 GPa, 34.7 ± 6.90 GPa, 29.5 ± 4.82 GPa, 83.5 ± 8.93 GPa, and 37.0 ± 10.9 GPa, respectively. Table 4 shows the values for the engineering elastic moduli of the enamel specimens. The mean values ± SD for Young's moduli E_1 and E_3 are 71.7 ± 7.34 GPa and 69.2 ± 7.32 GPa, respectively; for Poisson's ratios υ_{12} and υ_{13} are 0.303 ± 0.098 and 0.248 ± 0.060, respectively; and for shear moduli G_{13} and G_{12} are 37.0 ± 10.9 GPa and 28.1 ± 4.35 GPa, respectively.

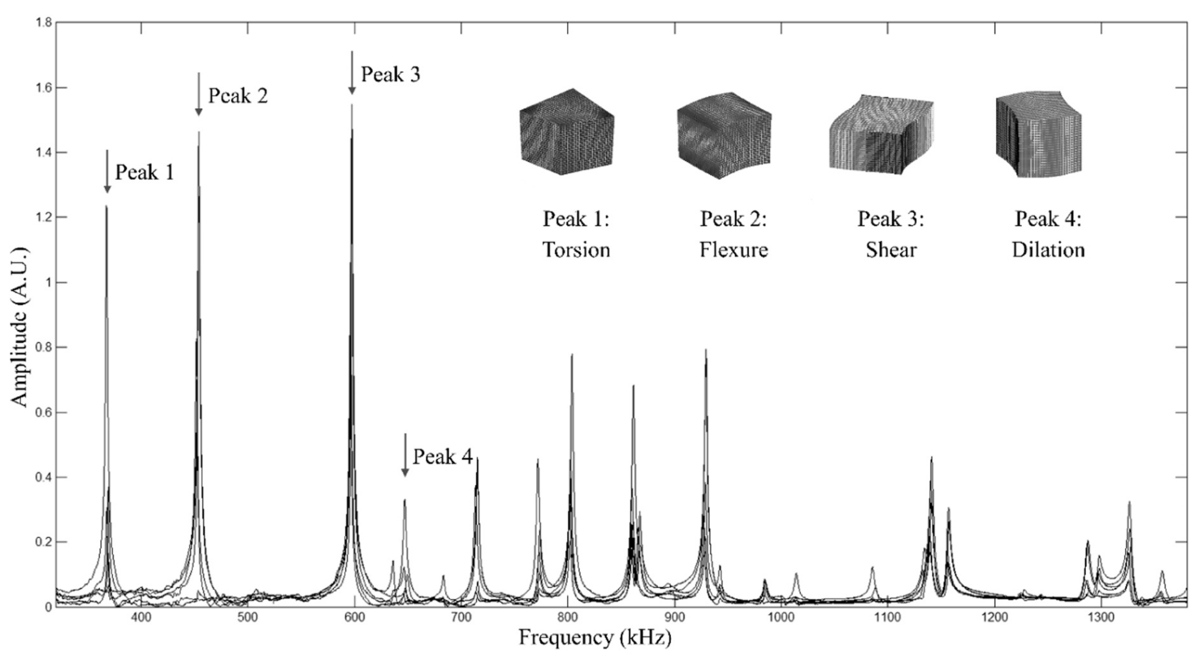

Fig. 4. Typical resonance spectra of the enamel specimen.

Table 4
Engineering elastic moduli of the enamel specimens.

No.	E_1 (GPa)	E_3 (GPa)	υ_{12}	υ_{13}	G_{13} (GPa)	G_{12} (GPa)
1	77.9	76.1	0.185	0.283	29.6	32.9
2	74.7	64.5	0.402	0.193	51.9	26.6
3	61.5	80.0	0.430	0.180	27.3	21.5
4	80.5	67.6	0.217	0.299	32.6	33.0
5	65.4	66.3	0.312	0.215	30.7	26.9
6	70.1	60.7	0.273	0.320	50.0	27.5
Mean	71.7	69.2	0.303	0.248	37.0	28.1
SD	7.34	7.32	0.098	0.060	10.9	4.35

4. Discussion

Researchers have used a variety of measurement techniques to obtain elastic properties of dental materials (Bowen and Rodriguez, 1962; Ye et al., 1994; Stanford et al., 1958; Craig et al., 1961; Zhang et al., 2014; Habelitz et al., 2001; Zhou and Hsiung, 2006; He et al., 2006; Watanabe et al., 2004; Ng et al., 1989; Gilmore et al., 1970; Lees and Rollins, 1972). However, due to the small size of human enamel or dentin specimens, accurate measurement of their elastic properties remains challenging. The limitations of the measurement techniques have led to large differences in the measurement results. As one of the most accurate methods to measure the stiffness of high Q solid materials (Bernard et al., 2013, 2014, 2015; Migliori and Maynard, 2005; Migliori and Sarrao, 1997; Migliori et al., 1993; Kinney et al., 2003, 2004; Fan et al., 2017) for small-sized specimens, RUS was applied to measure the stiffness of six small-sized human enamel specimens in this study, which is believed to be the first study to investigate the anisotropic elastic properties of enamel using this method.

Stiffness constants and engineering elastic moduli (Young's moduli, shear moduli, and Poisson's ratios), are the primary parameters for characterizing the elastic properties of enamel. Due to the difference in microstructures and symmetries of different materials, the number of independent stiffness constants for each material also varies. For example, an isotropic material has two independent stiffness constants, a transverse isotropic material has five independent stiffness constants, and an orthotropic material has nine independent stiffness constants. Similarly, the elastic properties of enamel are closely related to its microstructure and symmetry. For simplification, it has been generally assumed that enamel is isotropic (Bowen and Rodriguez, 1962; Ye et al., 1994; Stanford et al., 1958; Craig et al., 1961; Zhang et al., 2014; Habelitz et al., 2001). Considering the hierarchical assembled structure of human enamel proposed by Cui et al., the enamel prisms on the enamel surface are radially arranged in parallel, which presents a higher hardness and elastic modulus (Cui and Ge, 2007). As the depth increases, the orientation and alignment of enamel prisms change to curved crosses, which leads to reduced values of the mechanical properties. To describe the enamel materials more accurately, Wen et al. first assumed that enamel specimens are transversely isotropic based on the hierarchical structure and have five independent stiffness constants C_{11}, C_{12}, C_{13}, C_{33}, and C_{44} (Wen et al., 2014). This study also assumed that the specimens are transversely isotropic so that RUS is highly appropriate to estimate the five constants of the enamel specimens.

Comparing the resonance ultrasound spectra of the enamel specimens from this study (Fig. 4) with the resonance ultrasound spectra recorded for a dentin specimen in a previous study [(Fan et al., 2017), Fig. 2], the resonant peaks of enamel were found to be sharper and the overlaps between the peaks were found to be smaller, reflecting a higher Q value of enamel compared to dentin. Consequently, experimental resonant frequencies can be extracted with less ambiguity in the case of enamel.

Compared to the stiffness constants of dentin similarly calculated by the RUS method (Kinney et al., 2003, 2004; Fan et al., 2017), the stiffness constants of enamel were higher, which might be attributed to the higher mineralization of enamel and a denser and less porous material structure of enamel material. This result was consistent with previous researches (Ye et al., 1994; Stanford et al., 1958).

Despite an extensive literature review, there is no data found where experimental measurement of the actual stiffness constants of pure enamel material occurred under transversely isotropic conditions. Wen et al. used FEA to estimate the five stiffness constants of enamel, yielding values of 82.96 GPa, 36.04 GPa, 34.66 GPa, 92.89 GPa, and 22.90 GPa, respectively (Wen et al., 2014). All of Wen's stiffness constants were consistent with the measurement results in this study, except for C_{44}, which was higher in this study.

As discussed, the values of Young's moduli of human enamel obtained in previous studies vary widely. The diversity of the results may come from the use of different measurement methods. Young's modulus measurement results in this study were in the range of 60.7–80.5 GPa, which was consistent with the results of Stanford et al. (1958), but with less measurement deviation. In addition, Poisson's ratios υ_{12} (0.33) and υ_{13} (0.25) and shear modulus G_{12} (24.8 GPa) measured by Wen et al. (2014) with FEA were consistent with the measurement results of this study. The reason for the smaller G_{13} measured by Wen et al. compared to this study might be from their hypothesis of a simple enamel model, which did not capture the complexity of the actual enamel structure.

For Poisson's ratio υ_{12} and the shear modulus G_{13}, the differences among the specimens were about 30%. The main reason might be the difference in characteristics between each specimen, the different cutting sites among the specimens, as well as the preparation of the enamel specimens.

Due to the brittleness of enamel, it is difficult to make specimens that are pure enamel. The enamel specimens could contain some dentin or small defects (Cuy et al., 2002; Stanford et al., 1958). Moreover, due to the small size of the specimen, a very high geometrical quality of the enamel specimen is not practicable, as shown in Fig. 3. These shape imperfections would result in errors in the forward model for calculating the theoretical value of the resonant frequencies (Cai et al., 2017).

To achieve more accurate measurements of elastic properties of human enamel, future work is needed by using more accurate processing equipment to prepare more regular and pure enamel specimens to reduce the theoretical calculation error, and using another theoretical frequency estimation theory, such as FEA, to relax the size and shape requirements of the enamel specimens.

It should be noted that only a limited number of specimens were measured, so only preliminary results are shown. More studies are required to strengthen the conclusions.

In conclusion, RUS is an effective method to measure the engineering elastic moduli of small-sized enamel specimens. The results of this study pertaining to the stiffness constants and elastic moduli of enamel can be used to understand the elastic properties of dental materials and provide valuable information for dental material development and oral mechanics research.

Acknowledgements

This work was supported by the National Natural Science Foundation of China [Grant nos. 31570945 and 11772037].

Declaration of interest

None.

References

Bernard, S., Grimal, Q., Laugier, P., 2013. Accurate measurement of cortical bone elasticity tensor with resonant ultrasound spectroscopy. J. Mech. Behav. Bio Mater. 18, 12–19.

Bernard, S., Grimal, Q., Laugier, P., 2014. Resonant ultrasound spectroscopy for viscoelastic characterization of anisotropic attenuative solid materials. J. Acoust. Soc. Am. 135 (5), 2601–2613.

Bernard, S., Marrelec, G., Laugier, P., Grimal, Q., 2015. Bayesian normal modes identification and estimation of elastic coefficients in resonant ultrasound spectroscopy. Inverse Probl. 31. https://doi.org/10.1088/0266-5611/31/6/065010.

Bowen, R.L., Rodriguez, M.S., 1962. Tensile strength and modulus of elasticity of tooth structure and several restorative materials. J. Am. Dent. Assoc. 64 (3), 378–387.

Cai, X., Peralta, L., Gouttenoire, P., Olivier, C., Peyrin, F., Laugier, P., Grimal, Quentin, 2017. Quantification of stiffness measurement errors in resonant ultrasound spectroscopy of human cortical bone. J. Acoust. Soc. Am. 142, 2755–2765.

Craig, R.G., Peyton, F.A., Johnson, D.W., 1961. Compressive properties of enamel, dental cements, and gold. J. Dent. Res. 40 (5), 936–945.

Cui, F.Z., Ge, J., 2007. New observations of the hierarchical structure of human enamel, from nanoscale to microscale. J. Tissue Eng. Regen. Med. 1 (3), 185–191.

Cuy, J.L., Mann, A.B., Livi, K.J., Teaford, M.F., Weihs, T.P., 2002. Nanoindentation mapping of the mechanical properties of human molar tooth enamel. Arch. Oral Biol. 47 (4), 281–291.

Fan, F., Wang, R., Feng, D., Zhang, Q., Niu, H., 2017. The elasticity coefficients measurement of human dentin based on RUS. Biomed. Res. Int. https://doi.org/10.1155/2017/7852971.

Gilmore, R.S., Pollack, R.P., Katz, J.L., 1970. Elastic properties of bovine dentine and enamel. Arch. Oral Biol. 15 (8), 787–796.

Habelitz, S., Marshall, S.J., Marshall Jr, M.G., Balooch, M., 2001. Mechanical properties of human dental enamel on the nanometre scale. Arch. Oral Biol. 46 (2), 173–183.

He, L.H., Swain, M.V., 2008. Understanding the mechanical behaviour of human enamel from its structural and compositional characteristics. J. Mech. Behav. Bio Mater. 1 (1), 18–29.

He, L.H., Fujisawa, N., Swain, M.V., 2006. Elastic modulus and stress-strain response of human enamel by nano-indentation. Biomaterials 27 (24), 4388–4398.

Kinney, J.H., Marshall, S.J., Marshall, G.W., 2003. The mechanical properties of human dentin: a critical review and re-evaluation of the dental literature. Crit. Rev. Oral Biol. Med. 14 (1), 13–29.

Kinney, J.H., Gladden, J.R., Marshall, G.W., Marshall, S.J., So, J.H., Maynard, J.D., 2004. Resonant ultrasound spectroscopy measurements of the elastic constants of human dentin. J. Biomech. 37 (4), 437–441.

Lees, S., Rollins, F.R., 1972. Anisotropy in hard dental tissues. J. Biomech. 5 (6), 557–564.

Migliori, A., Maynard, J.D., 2005. Implementation of a modern resonant ultrasound spectroscopy system for the measurement of the elastic moduli of small solid specimens. Rev. Sci. Instrum. 76 (12). https://doi.org/10.1063/1.2140494.

Migliori, A., Sarrao, J.L., 1997. Resonant Ultrasound Spectroscopy: Applications to Physics, Materials Measurements, and Nondestructive Evaluation. Wiley, New York.

Migliori, A., Sarrao, J.L., Visscher, W.M., Bell, T.M., Lei, M., Fisk, Z., Leisure, R.G., 1993. Resonant ultrasound spectroscopic techniques for measurement of the elastic moduli of solids. Physica B 183, 1–24.

Ng, S.Y., Payne, P.A., Cartledge, N.A., Ferguson, M.W.J., 1989. Determination of ultrasonic velocity in human enamel and dentine. Arch. Oral Biol. 34 (5), 341–345.

Stanford, J.W., Paffenbarger, G.C., Kumpula, J.W., Sweeney, W.T., 1958. Determination of some compressive properties of human enamel and dentin. J. Am. Dent. Assoc. 57 (4), 487–495.

Watanabe, T., Miyazaki, M., Inage, H., Kurokawa, H., 2004. Determination of elastic modulus of the components at dentin-resin interface using the ultrasonic device. Dent. Mater. J. 23 (3), 361–367.

Wen, M., Zheng, J., Zhou, Z., 2014. Finite element analysis on effect of organic phase on mechanical properties of human tooth enamel. Lubr. Eng. 39 (7), 21–25 (in Chinese).

Ye, D., Su, Y., Wang, B., Xiang, Y., Zhao, Y., Du, C., Wei, Z., Lu, X., Lu, Y., 1994. Measurement of Poisson's ratio of human enamel. West China J. Stomatol. 4, 295–297.

Zhang, Y.R., Du, W., Zhou, X.D., Yu, H.Y., 2014. Review of research on the mechanical properties of the human tooth. Int. J. Oral Sci. 6 (2), 61–69.

Zhou, J., Hsiung, L.L., 2006. Depth dependence of the mechanical properties of human enamel by nanoindentation. J. Biomed. Mater. Res. A 81A (1), 1–28.